

TRANSPORT OF POSITRONS IN THE INTERSTELLAR MEDIUM

W. Gillard¹, P. Jean¹, A. Marcowith², and K. Ferrière³

¹*C.E.S.R., CNRS/Université Paul Sabatier, Toulouse, France*

²*L.P.T.A. CNRS-UM2 Université Montpellier II, France*

³*L.A.T.T., CNRS/OMP, Toulouse France*

ABSTRACT

This work investigates some aspects of the transport of low-energy e^+ ($E_k \lesssim 1$ MeV) in the interstellar medium (ISM). We consider resonance interactions with magneto-hydrodynamic (MHD) waves above the resonance threshold. Below the threshold, collisions take over and deflect e^+ in their motion parallel to magnetic-field lines. Using Monte-Carlo simulations, we model the propagation and energy losses of e^+ in the different phases of the ISM until they annihilate. We suggest that e^+ produced in the disk by an old population of stars (SNIa, LMXB), with initial kinetic energies below 1 MeV, and propagating in the spiral magnetic field of the disk, can probably not penetrate the Galactic bulge.

Key words: Positrons; Diffusion process; Interstellar medium.

1. INTRODUCTION

The map of the 511 keV e^-e^+ annihilation emission, measured by the spectrometer SPI on board ESA's INTEGRAL observatory, indicates that e^+ annihilate mainly in the Galactic bulge, with a bulge-to-disk flux ratio $B/D \simeq 2 \pm 1$ [15]. Under the assumption that e^+ annihilate near their sources, this ratio provides severe constraints on the e^+ sources. The measured value of B/D does not correspond to any known distribution of astrophysical objects. The annihilation emission from the disk may be due to ^{26}Al and ^{44}Ti ejected by massive stars, but the origin of e^+ in the bulge is still a mystery. Jean et al. [14] suggested that e^+ produced in the bulge with energies lower than a few MeV do not escape and, therefore, annihilate in the bulge. Prantzos [16] argued that a ballistic transport of 1 MeV e^+ from the disk into the bulge via a regular dipolar magnetic field could explain a high B/D ratio.

The transport of e^+ is still poorly understood, but, as all charged particles, e^+ are sensitive to the Galactic electromagnetic field, the flows of interstellar matter and the interactions with gas particles. In this paper, we report on

preliminary results of e^+ transport in the Galaxy. Section 2 describes the effects of interactions with Alfvén waves. Section 3 presents the model of collisional diffusion. The implications of our model and the other possible processes of diffusion are discussed in Section 4.

2. INTERACTIONS WITH ALFVÉN WAVES

In this section, we restrict the present analysis to the interactions between e^+ and Alfvén waves, usually assumed to be the main transport agent in the ISM. The effects of e^+ interactions with magnetosonic waves are postponed to a future work.

Regardless of the origin of Alfvén waves, the strong damping of Alfvén waves above the proton cyclotron frequency implies an energy threshold (K_{QL}) to the resonance condition. In the case of e^+ , this condition can be satisfied only if [14]

$$\gamma\beta \geq 12.85 \times 10^{-3} \frac{B_{\mu\text{G}}}{\sqrt{n_{\text{cm}^{-3}}}}, \quad (1)$$

where γ is the e^+ Lorentz factor, β the e^+ velocity divided by the speed of light, B the magnetic-field strength and n the total particle density of the considered phase. When e^+ are in resonance with Alfvén waves, we use quasilinear theory to derive the diffusion coefficient, which enables us to estimate the distance travelled by e^+ (see Equation 7 in [14]).

Note, however, that when the amplitudes of magnetic fluctuations become comparable to the strength of the mean magnetic field, quasilinear theory gives a crude description of e^+ transport. This particular aspect will be addressed in a future paper.

3. INTERACTIONS WITH GAS PARTICLES

Below the quasilinear energy threshold, the resonance condition is not satisfied. Therefore, we assume that e^+ propagate in a collisional regime. We calculate the

distance travelled by e^+ using Monte-Carlo simulations which take into account the physics of e^+ interactions with gas particles and their associated cross sections [2, 3, 7, 8, 20]. The present analysis is restricted to a neutral hydrogen gas ($n = n_{\text{HI}}$) and a fully ionized hydrogen gas ($n = n_{e^-} + n_{\text{HII}}$). The effects of the ionization fraction and metallicity will be presented elsewhere. Since the n -dependence of the quantities of interest is known analytically, we may arbitrarily adopt $n = 1 \text{ cm}^{-3}$.

The medium is assumed to be pervaded by a homogeneous magnetic field \vec{B}_0 , directed along the z axis and having a strength of $5 \mu\text{G}$ (in agreement with the typical value measured in the Galactic disk). Each e^+ travels along magnetic-field lines and describes a helical orbit of radius equal to its Larmor radius. When a e^+ interacts with a gas particle, its trajectory is deflected and the e^+ loses a fraction of its energy or it annihilates. Each simulation is performed using a total number of e^+ ranging between 5×10^3 and 2×10^4 . The initial pitch angle is chosen randomly according to an isotropic distribution in the half-space $z \geq 0$. In this regime, the distance travelled along magnetic-field lines by e^+ with a given initial energy does not depend on the magnetic-field strength. In the next sections, the results of our simulations are presented for e^+ with an initial kinetic energy of 3 keV.

3.1. Transport in a neutral medium

In a neutral medium, e^+ lose energy through ionization and excitation of atoms and through elastic scattering with atoms. They annihilate with bound e^- either directly or after forming a positronium in flight by charge exchange. To estimate the distance travelled by e^+ in a neutral medium, we distinguish three periods during the e^+ lifetime:

1. The slowing-down period.

When the kinetic energy of e^+ lies between the *quasilinear threshold* and the charge exchange threshold (6.8 eV in H), e^+ lose energy mainly through ionization and/or excitation, and $\simeq 98\%$ of them annihilate in flight, in quite good agreement with [7]. In Figure 1, we show the final distribution of e^+ parallel to magnetic-field lines. This distribution is obtained when the e^+ energy reaches the charge exchange threshold or when e^+ annihilate. The distribution provides an estimate of the average distance travelled by e^+ along magnetic-field lines. It can be fitted by a Gaussian, using χ^2 minimization, with an average distance $\langle z \rangle \simeq (0.886 \pm 0.005)/n_{\text{cm}^{-3}}$ pc and a spatial dispersion $\langle z^2 \rangle^{1/2} \simeq (0.707 \pm 0.003)/n_{\text{cm}^{-3}}$ pc, obtained after an average slowing-down time $\langle t \rangle \simeq 86/n_{\text{cm}^{-3}}$ yr.

The distance travelled by e^+ during this period does not depend on the temperature of the gas, since their kinematic energy is always larger than the thermal energy of the gas ($\lesssim 1 \text{ eV}$).

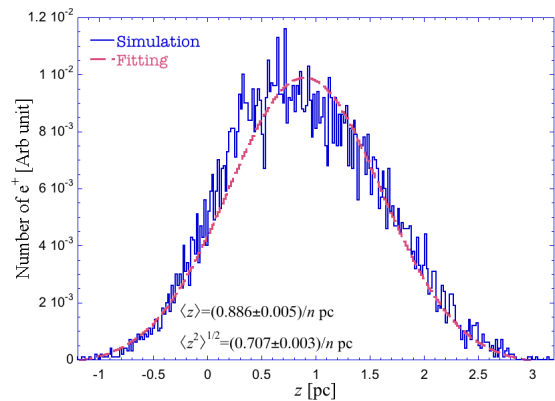


Figure 1. Spatial distribution of e^+ parallel to magnetic-field lines at the final stage of the slowing-down period. The initial e^+ kinetic energy is 3 keV and the total gas density is $n = 1 \text{ cm}^{-3}$.

Note that, in a neutral medium, Alfvén waves could be strongly damped by ambipolar diffusion. In this case, the slowing-down period of collisional diffusion would start at higher energies, maybe even at the injection energy of e^+ . Starting collisional diffusion with an initial e^+ kinetic energy of 1 MeV and using the theory of inelastic scattering [6], we obtain $\langle z \rangle \simeq 4.0/n_{\text{cm}^{-3}}$ pc, $\langle z^2 \rangle^{1/2} \simeq 7.4/n_{\text{cm}^{-3}}$ pc and an averaged slowing-down time $\simeq 220/n_{\text{cm}^{-3}}$ yr.

2. The thermalization period.

e^+ below the energy threshold for charge exchange lose energy elastically until their kinetic energy drops to that of gas particles. We obtain the spatial distribution parallel to magnetic-field lines that is shown in Figure 2. The thermalization time is $\simeq 10^4/n_{\text{cm}^{-3}}$ yr. Using χ^2 minimization, we can fit the curve by a Gaussian with an average distance $\langle z \rangle \simeq (4 \pm 6) \times 10^{-3}/n_{\text{cm}^{-3}}$ pc and a spatial dispersion $\langle z^2 \rangle^{1/2} \simeq (0.19 \pm 0.01)/n_{\text{cm}^{-3}}$ pc. During this period, e^+ annihilation is possible, but negligible ($\leq 1\%$). The effect of the gas temperature is also found to be negligible. Between 8000 K and 10 K, the difference in $\langle z^2 \rangle^{1/2}$ is less than 8%.

3. The thermalized period.

During this period, the kinetic energy of e^+ is comparable to the thermal energy of gas particles and e^+ scatter elastically with atoms. On average, there is neither gain nor loss in energy and e^+ diffuse over a distance $\lambda = \sqrt{2D\tau}$ along magnetic-field lines until they annihilate directly with bound e^- (τ is the e^+ lifetime [7]). Given in Table 1 are the values of the diffusion coefficient D parallel to magnetic-field lines that we computed for the different ISM phases. It has to be noted that both D and τ depend on the gas temperature.

In agreement with the equation of motion of e^+ in a magnetic field, the magnetic-field strength influences only the

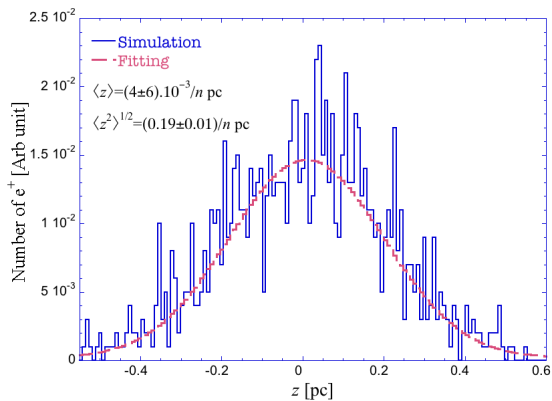


Figure 2. Spatial distribution of e^+ parallel to magnetic-field lines at the final stage of the thermalization period. The initial e^+ kinetic energy is equal to the charge-exchange threshold and the total gas density is $n = 1 \text{ cm}^{-3}$.

ISM phase	Temperature	Diffusion coefficient
Molecular	20 K	$2.1 \times 10^{21} / n \text{ cm}^2 \cdot \text{s}^{-1}$
Cold neutral	100 K	$1.2 \times 10^{21} / n \text{ cm}^2 \cdot \text{s}^{-1}$
Warm neutral	8000 K	$5.6 \times 10^{23} / n \text{ cm}^2 \cdot \text{s}^{-1}$
Warm ionized	8000 K	$4.4 \times 10^{17} / n \text{ cm}^2 \cdot \text{s}^{-1}$
Hot ionized	10^6 K	$7.8 \times 10^{22} / n \text{ cm}^2 \cdot \text{s}^{-1}$

Table 1. Estimated values of the parallel diffusion coefficient in the thermalized period in the different ISM phases.

perpendicular transport. In all three periods listed above, distances traveled perpendicular to magnetic-field lines are found to be negligible ($d_{\perp} \lesssim 10^{-10} / n_{\text{cm}^{-3}} \text{ pc}$).

3.2. Transport in an ionized medium

In an ionized medium, e^+ lose energy through Coulomb scattering with ions and free e^- . They annihilate with free e^- either directly or after forming a positronium by radiative combination [7]. Here, we model Coulomb interactions according to [11] and [2]. In contrast to propagation in a neutral medium, propagation here depends on the gas temperature. To estimate e^+ transport in an ionized medium, we divide the e^+ lifetime into two periods:

1. The slowing-down or thermalization period.

During slowing-down, e^+ lose energy through Coulomb scattering, and a negligible fraction ($\lesssim 1\%$) of e^+ annihilate. In Figure 3, we show the spatial distribution of e^+ parallel to magnetic-field lines at the end of the slowing-down period, i.e. at a time $\sim 25 / n_{\text{cm}^{-3}} \text{ yr}$. The average distance $\langle z \rangle$ travelled by e^+ and the spatial dispersion $\langle z^2 \rangle^{1/2}$ of the distribution are indicated in Table 2, for both the warm ionized and the hot ionized phases.

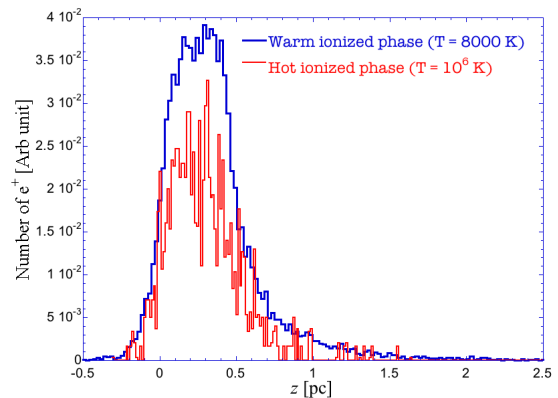


Figure 3. Spatial distribution of e^+ parallel to magnetic-field lines at the end of the slowing-down period, in the warm ionized (upper blue line) and the hot ionized (lower red line) phases. The initial e^+ kinetic energy is 3 keV and the total gas density is $n = 1 \text{ cm}^{-3}$.

ISM phase	$\langle z \rangle$	$\langle z^2 \rangle^{1/2}$
Warm ionized	$0.34 / n_{\text{cm}^{-3}} \text{ pc}$	$0.35 / n_{\text{cm}^{-3}} \text{ pc}$
Hot ionized	$0.30 / n_{\text{cm}^{-3}} \text{ pc}$	$0.24 / n_{\text{cm}^{-3}} \text{ pc}$

Table 2. Average distance $\langle z \rangle$ travelled by e^+ during the slowing-down period and spatial dispersion of the distribution $\langle z^2 \rangle^{1/2}$ in the warm ionized and hot ionized phases. n is the total gas density.

2. The thermalized period.

During this period, the kinetic energy of e^+ is comparable to the thermal energy of gas particles and e^+ interact with e^- via Coulomb scattering. On average, there is neither gain nor loss in energy and e^+ diffuse over a distance $\lambda = \sqrt{2D\tau}$ along magnetic-field lines until they annihilate with free e^- . Here, too, the values of the diffusion coefficient D parallel to magnetic-field lines are given in Table 1.

As in the case of a neutral medium, diffusion perpendicular to magnetic-field lines is found to be negligible ($d_{\perp} \lesssim 2 \times 10^{-11} / n_{\text{cm}^{-3}} \text{ pc}$).

4. DISCUSSION AND CONCLUSION

In this section, we discuss the effects of the transport of e^+ produced around 1 MeV by an old stellar population (type Ia supernovae, low-mass X-ray binaries, ...) in the Galactic disk. Table 3 gives the average distances travelled by e^+ at different locations in the Galactic disk ($r \gtrsim 3 \text{ kpc}$), as computed with the method presented in the previous sections. Because e^+ follow magnetic-field lines, we start by describing the magnetic-field properties in the disk.

The current observational status, based on studies of the Galactic synchrotron emission [1] and of Faraday rotation

Galactic height	ISM phase	Total density (cm^{-3})	K_{QL} (keV)	d_{QL} (pc)	d_{Col} (pc)
$z = 0$ kpc	Molecular	$(10^2 - 10^6)$	$\lesssim 10^{-2}$	$\lesssim 4$	$\lesssim 10^{-3}$
	Cold neutral	$(20 - 50)$	$(5.3 - 2.1)10^{-2}$	$(5 - 10)$	$\lesssim 10^{-2}$
	Warm neutral	$(0.2 - 0.5)$	$(5.3 - 2.1)$	$(50 - 80)$	$(5 - 10)$
$z = 0.3$ kpc	Warm ionized	~ 0.2	~ 5.2	~ 40	$\lesssim 1$
	Hot ionized	~ 0.002	~ 380	~ 250	~ 600

Table 3. Average distances travelled by e^+ with an initial kinetic energy of 1 MeV in the quasi-linear (d_{QL}) and collisional (d_{Col}) regimes, at different locations in the Galactic disk. The total particle densities are derived from [4, 5]

measures [9, 10, 12, 18, 19], is basically the following: The interstellar magnetic field has uniform (large-scale) and turbulent (small-scale) components of comparable strengths ($\simeq 1.5 \mu\text{G}$ and $\sim 5 \mu\text{G}$, respectively in the Solar vicinity). The direction of the uniform magnetic field is nearly horizontal in most of the Galactic disk, and on the whole, the azimuthal component dominates. The uniform magnetic field probably has a spiral pattern, but it is not known whether this spiral is axisymmetric, bisymmetric, or a mixture of different azimuthal modes. The strength of the uniform magnetic field increases smoothly toward the Galactic center, reaching at least $4 \mu\text{G}$ at $r \simeq 4$ kpc. Along the vertical, the uniform field strength decreases away from the midplane, probably following a two-layer structure with respective scale heights ~ 200 pc and $\sim 2 - 4$ kpc.

The old stellar population is more spread out along the vertical than neutral gas. Here, we assume for simplicity that at $z \sim 0.3$ kpc the ISM is fully ionized. In accordance with the ISM distribution [4, 5], we adopt $n \sim 0.2 \text{ cm}^{-3}$ for the warm ionized phase and $n \sim 0.002 \text{ cm}^{-3}$ for the hot ionized phase. With an initial kinetic energy ~ 1 MeV, e^+ start propagating by diffusion on Alfvén waves until their kinetic energy falls below ~ 5.2 keV in the warm ionized phase and ~ 380 keV in the hot ionized phase. While e^+ are transported by Alfvén waves, they travel an average distance ~ 40 pc in the warm ionized phase and ~ 250 pc in the hot ionized phase. Below the resonance threshold, e^+ propagate by collisions until they annihilate. The average distance travelled in the collisional diffusion regime is $\lesssim 1$ pc in the warm ionized phase and ~ 600 pc in the hot ionized phase (see Table 3). Consequently, the maximum average distance travelled by e^+ before annihilation is ~ 850 pc. We also estimate that the maximum possible distance travelled by a typical e^+ is ~ 1 kpc. Assuming a spiral magnetic field in the Galactic disk, we then conclude that e^+ produced at Galactocentric radius $r \gtrsim 3$ kpc can not reach the Galactic bulge.

Note that in the current model, e^+ follow the average magnetic-field lines. However, in the Galactic disk, superbubbles and supernova remnants generate turbulence that can drive magnetic-field lines at high altitude ($\gtrsim 1$ kpc). There, e^+ are in a low-density medium where complex magnetic effects could significantly change the transport of e^+ . Galactic winds could also transport e^+ advectively. In the Galactic center, a number of young massive stellar clusters blowing powerful winds have been observed [13, 17]. Such points will be addressed

in a future work.

ACKNOWLEDGMENTS

A special thank to the local organizing committee of the 6th INTEGRAL workshop. W. Gillard would like to acknowledge J. P. Roques for the financial support.

REFERENCES

- [1] Beuermann K., Kanbach G. and Berkhuijsen E. M., 1985, A&A 153:17
- [2] Butler S. T. and Buckingham M. J., 1962, Phys Rev 126:1
- [3] Charlton M. and Humberston J. W., 2001, *Positron Physics*, in Cambridge Monographs on Atomic, Molecular and Chemical Physics
- [4] Ferrière K., 1998, ApJ 497:759
- [5] Ferrière K., 2001, Rv Modern Phys. 73:1031
- [6] Gryziński M., 1965, Phys Rev A 138:336
- [7] Guessoum N., Jean P. and Gillard W., 2005, A&A 436:171
- [8] Gould R. J., 1989, ApJ 344:232
- [9] Han J. L., Manchester R. N. and Qiao G. J., 1999, MNRAS 306:371
- [10] Han J. L., Manchester R. N., Lyne A. G., et al. 2006, ApJ 642:868
- [11] Huba J. D., 1994, NRL/PU/6790D 94:265
- [12] Inoue M. and Tabara, H., 1981, PASJ 33:603
- [13] Ipavich F. M., 1975, ApJ 196:107
- [14] Jean P., Knödseder J., Gillard W., et al. 2006, A&A 445:579
- [15] Knödseder J., Jean P., Lonjou V., et al. 2005, A&A 441:513
- [16] Prantzos N., 2006, A&A 449:878
- [17] Portegies-Zwart S. F., Makino J., McMillan S. L. W., et al. 2001, ApJ 546:L101
- [18] Rand R. J., Lyne A. G., 1994, MNRAS 268:497
- [19] Simard-Normandin M., Kronberg P. P., 1980, ApJ 242:74
- [20] Wallyn P., Durouchoux Ph., Chapuis C., et al. 1994, ApJ 422:610